Int. J. Heat Mass Transfer Vol. 30, No. 6, pp. 1119–1131, 1987
Printed in Great Britain

0017–9310/87 $3.00+0.00
Pergamon Journals Ltd.

Vertical mixed convection flow about a horizontal line source of heating or cooling

GRAHAM WILKS
Department of Mathematics, University of Keele, Keele, Staffordshire ST5 5BG, U.K.
and
ROLAND HUNT
Department of Mathematics, University of Strathclyde, Glasgow G1 1XH, U.K.

(*Received* 1 *August* 1986)

Abstract—The vertical mixed convection flow of a uniform stream, about a horizontal line source generating favourable buoyancy effects, may be characterized by an evolution between a weak and strong plume. This appraisal of the developing flow field provides the basis for an efficient formulation of the problem. Comprehensive solutions within this framework are obtained for a wide range of Prandtl numbers. In contrast the vertical mixed convection flow about a horizontal line source resulting in adverse buoyancy forces may be expected ultimately to display stagnation. Numerical solutions of the boundary layer equations governing this adverse case reveal that the anticipated stagnation is accompanied by a singular behaviour characterized by unbounded growth of the shear layer.

1. INTRODUCTION

THE MIXED convection flow of a uniform stream about a horizontal line source of heat has recently been discussed by Afzal [1]. In contrast to earlier workers, Wood [2] and Wesseling [3], who analysed equations based upon an Oseen linearization of the Navier–Stokes equations, Afzal considers the full non-linear, governing boundary layer equations. Using series extension techniques, forcasts for various features of the flow were obtained from regular series solutions, valid in the vicinity of the heat source, for a Prandtl number of 0.72. Haaland and Sparrow [4] have subsequently commented on the limitations of this investigation and have extended the discussion, both theoretically and numerically, to Prandtl numbers ranging from $O(1)$ to infinity. In particular Haaland and Sparrow develop algebraic relations, valid for that range of Prandtl numbers, which accurately predict the centre-line velocity and temperature distributions when buoyancy effects are positive with respect to the oncoming uniform stream.

Although it is acknowledged that the flow under examination will evolve towards the similarity state associated with the pure free convection plume, Haaland and Sparrow do not exploit this inherent structure in their numerical solutions. As a result large numbers of grid points (~ 1500) are required to achieve the required accuracy over the semi-infinite region downstream of the heat source. Moreover, these authors do not proceed to examine the flow associated with a source whose buoyancy is negative with respect to the oncoming stream. In this situation it is to be expected that the buoyancy interaction with the uniform stream will lead to a stagnation of the flow. Indeed Afzal's work supports this conjecture and identifies the location of such a stagnation point. An unusual feature of the predicted temperature distribution in the vicinity of stagnation is the presence of a temperature maximum away from the axis of symmetry. In view of the susceptibility of series extension techniques to round off error one is led to question whether or not this is a physical feature of the flow or a spurious prediction of the series representation.

In the work that follows we present a comprehensive re-examination of the prescribed flow. In the first instance we introduce an alternative numerical formulation of the positively buoyant case. The formulation exploits the evolution of the flow between known similarity states. An efficient algorithm presented by Hunt and Wilks [5] to handle precisely this circumstance is used to obtain numerical solutions for a wide range of Prandtl numbers between zero and infinity. Flow characteristics are extracted from the solutions and shown to coincide downstream with those of the pure plume as presented by Fujii *et al.* [6]. Further numerical solutions are then obtained for the case of the negatively buoyant heat source. The solutions display the anticipated stagnation. As the numerical solution approaches the stagnation point there is evidence of a singular breakdown of the governing equations characterized by unbounded growth of the boundary layer thickness. Certain structural features of the singular behaviour are extracted from the numerical solution which may provide the basis for a local analysis of the precise nature of the singularity. It is noteworthy that as the

NOMENCLATURE

c_p	specific heat at constant pressure
$f, \bar{f}, \tilde{f}$	non-dimensional stream functions at small ξ, large ξ and for continuous transformation, respectively
g	acceleration due to gravity
Gr_x	local Grashof number
J	normalized excess momentum flux
M	normalized excess mass flux
Q	heat released per unit length of thermal source
Re_x	local Reynolds number
T	temperature
T_∞	ambient temperature
(x, y)	coordinates measured vertically from line source and normal to the axis of symmetry, respectively
(u, v)	velocity components
U_∞	free stream velocity.

Greek symbols

β	coefficient of thermal expansion
$\bar{\delta}$	half-width of velocity variation
$\bar{\delta}_T$	half-width of temperature variation
$\eta, \bar{\eta}, \tilde{\eta}$	non-dimensional normal coordinate at small ξ, large ξ and for continuous transformation, respectively
$\theta, \bar{\theta}, \tilde{\theta}$	non-dimensional temperature at small ξ, large ξ and for continuous transformation, respectively
κ	coefficient of thermometric conductivity
ν	coefficient of kinematic viscosity
ξ	non-dimensional axial coordinate
ρ	density of fluid
σ	Prandtl number
ψ	stream function.

stagnation point is approached there is no indication of the aforementioned temperature maximum away from the axis of symmetry.

2. THE GOVERNING EQUATIONS

When a uniform stream of velocity U_∞ and T_∞ flows vertically past a horizontal line source of heat, the boundary layer equations for the flow are

$$\frac{\partial u}{\partial x} + \frac{\partial v}{\partial y} = 0 \tag{1}$$

$$u\frac{\partial u}{\partial x} + v\frac{\partial u}{\partial y} = \nu\frac{\partial^2 u}{\partial y^2} \pm g\beta(T - T_\infty) \tag{2}$$

$$u\frac{\partial T}{\partial x} + v\frac{\partial T}{\partial y} = \kappa\frac{\partial^2 T}{\partial y^2}. \tag{3}$$

Here (u, v) are velocity components associated with coordinates (x, y) measured vertically from the heat source and normal to the axis of symmetry; T is the temperature and g, β, ν and κ are the acceleration due to gravity, the coefficient of thermal expansion, the kinematic viscosity and thermometric conductivity, respectively. The Boussinesq approximation is assumed to hold and the plus or minus signs in equation (2) correspond to a positively or negatively buoyant source.

The flow is assumed to be symmetric about the x-axis and hence

$$v = \frac{\partial u}{\partial y} = \frac{\partial T}{\partial y} = 0 \qquad \text{on } y = 0 \tag{4}$$

whilst ambient conditions require

$$u \to U_\infty, \quad T \to T_\infty \qquad \text{as } y \to \infty. \tag{5}$$

An energy conservation constraint is obtained from equation (3) in the form

$$\rho c_p \int_{-\infty}^{\infty} u(T - T_\infty)\,dy = Q \tag{6}$$

where c_p is the specific heat at constant pressure, ρ the density of the fluid and Q is the heat released per unit length of thermal source. Accordingly the energy transported across any plane is exactly that introduced into the flow by the source at $x = 0$.

3. NUMERICAL FORMULATION—POSITIVE BUOYANCY

The relative local magnitudes of the physical mechanisms in the flow are characterized by the non-dimensional coordinate

$$\xi = \frac{Gr_x^2}{Re_x^5} = \frac{(g\beta Q)^2 x}{(\rho c_p)^2 \nu U_\infty^5} \tag{7}$$

where Gr_x and Re_x are the local Grashof and Reynolds numbers, respectively, given by

$$Gr_x = \frac{g\beta Q x}{\rho c_p \nu^3}; \qquad Re_x = \frac{U_\infty x}{\nu}. \tag{8}$$

The transformations, boundary conditions and conservation constraints appropriate to the limiting similarity states associated with $\xi \to 0$ and $\xi \to \infty$ are then:

Small ξ

$$\psi = (\nu U_\infty x)^{1/2} f(\xi, \eta);$$

$$T - T_\infty = \left(\frac{\nu}{U_\infty x}\right)^{1/2} \frac{Q}{\rho c_p \nu} \theta(\xi, \eta)$$

$$\eta = y\left(\frac{U_\infty}{\nu x}\right)^{1/2}$$

$$f(\xi, 0) = f_{\eta\eta}(\xi, 0) = \theta_\eta(\xi, 0) = 0$$

$$f_\eta \to 1, \qquad \theta \to 0 \qquad \text{as} \quad \eta \to \infty$$

$$\int_{-\infty}^{\infty} f_\eta \theta \, d\eta = 1. \tag{9}$$

Large ξ

$$\psi = \nu\left(\frac{g\beta Q}{\rho c_p \nu^3}\right)^{1/5} x^{3/5} \bar{f}(\xi, \bar{\eta});$$

$$T - T_\infty = \left(\frac{g\beta Q}{\rho c_p}\right)^{4/5} \frac{1}{\nu^{2/5} g\beta x^{3/5}} \bar{\theta}(\xi, \bar{\eta})$$

$$\bar{\eta} = \frac{y}{x^{2/5}}\left(\frac{g\beta Q}{\rho c_p \nu^3}\right)^{1/5}$$

$$\bar{f}(\xi, 0) = \bar{f}_{\bar{\eta}\bar{\eta}}(\xi, 0) = \bar{\theta}_{\bar{\eta}}(\xi, 0) = 0$$

$$\bar{f}_{\bar{\eta}} \to \xi^{-1/5}, \qquad \bar{\theta} \to 0 \qquad \text{as} \quad \bar{\eta} \to \infty$$

$$\int_{-\infty}^{\infty} \bar{f}_{\bar{\eta}} \bar{\theta} \, d\bar{\eta} = 1. \tag{10}$$

The continuous transformation algorithm of Hunt and Wilks [5] creates a single set of governing equations which effect a smooth transition between those transformed equations associated with equations (9) and (10). In this case the intermediate transformations are

$$\psi = (1 + \xi)^{1/10} (\nu U_\infty x)^{1/2} \tilde{f}(\xi, \tilde{\eta});$$

$$T - T_\infty = (1 + \xi)^{-1/10} \left(\frac{\nu}{U_\infty x}\right)^{1/2} \frac{Q}{\rho c_p \nu} \tilde{\theta}(\xi, \tilde{\eta}) \tag{11}$$

$$\tilde{\eta} = (1 + \xi)^{1/10} \left(\frac{U_\infty}{\nu x}\right)^{1/2} y$$

and the governing equations are

$$\tilde{f}_{\tilde{\eta}\tilde{\eta}\tilde{\eta}} + \left[\frac{1}{2} + \frac{\xi}{10(1 + \xi)}\right] \tilde{f}\tilde{f}_{\tilde{\eta}\tilde{\eta}} - \frac{\xi}{5(1 + \xi)} \tilde{f}_{\tilde{\eta}}^2 = \xi[\tilde{f}_{\tilde{\eta}} \tilde{f}_{\tilde{\eta}\xi} - \tilde{f}_\xi \tilde{f}_{\tilde{\eta}\tilde{\eta}}] \tag{12}$$

$$\frac{1}{\sigma} \tilde{\theta}_{\tilde{\eta}\tilde{\eta}} + \left[\frac{1}{2} + \frac{\xi}{10(1 + \xi)}\right] \tilde{\theta}_{\tilde{\eta}} \tilde{f} + \left[\frac{1}{2} + \frac{\xi}{10(1 + \xi)}\right] \tilde{\theta} \tilde{f}_{\tilde{\eta}} = \xi[\tilde{f}_{\tilde{\eta}} \tilde{\theta}_\xi - \tilde{\theta}_{\tilde{\eta}} \tilde{f}_\xi] \tag{13}$$

to be solved subject to

$$\tilde{f}(\xi, 0) = \tilde{f}_{\tilde{\eta}\tilde{\eta}}(\xi, 0) = \tilde{\theta}_{\tilde{\eta}}(\xi, 0) \qquad \text{at} \quad \tilde{\eta} = 0$$

$$\tilde{f}_{\tilde{\eta}} \to \frac{1}{(1 + \xi)^{1/5}}, \qquad \tilde{\theta} \to 0 \qquad \text{as} \quad \tilde{\eta} \to \infty$$

$$\int_{-\infty}^{\infty} \tilde{f}_{\tilde{\eta}} \tilde{\theta} \, d\tilde{\eta} = 1. \tag{14}$$

The above parabolic system of equations may then be integrated straightforwardly as a set of five first-order differential equations using the Keller box [7] method. The integration is initiated by the known analytic solutions at $\xi = 0$, namely

$$\tilde{f}(0, \tilde{\eta}) = \tilde{\eta}; \quad \tilde{\theta}(0, \tilde{\eta}) = \left(\frac{\sigma}{4\pi}\right)^{1/2} \exp\left(-\frac{\sigma \tilde{\eta}^2}{4}\right) \tag{15}$$

where $\sigma = \nu/\kappa$ is the Prandtl number. As all derivatives in the method involve central differences it is possible to obtain highly accurate solutions. The accuracy of the results could be ascertained in three ways, (i) by comparing the results at $\xi \sim 10^{20}$ with known analytic solutions for $\sigma = 5/9$ and 2 for the pure free convection plume, (ii) from the convergence of the extrapolation and (iii) from the integral constraint of equations (14). As a consequence it is anticipated that results are accurate to six significant digits. In support of this assertion the numerical details of the present computation at $\xi \sim 10^{20}$ are compared in Table 1 with the accurate solutions of Fujii *et al.* [6] for the pure free convection plume.

4. RESULTS AND DISCUSSION—POSITIVE BUOYANCY

Some features of the numerical solutions have been extracted and illustrated. In Figs. 1–3 developing velocity and temperature profiles are contrasted for $\sigma = 0.1$, 1, and 10. A common grid has been used to emphasize the significant variations in the regions of influence of the source for varying Prandtl numbers. At low Reynolds number the regions of influence of velocity and temperature variations are comparable. As the Prandtl number increases however the region of the flow field affected by temperature variations diminishes relative to the region affected by velocity variations.

The progressive evolution from the uniform stream towards the pure free convection plume is also evident in Figs. 1–3. Centre-line velocities and temperatures are illustrated in Figs. 4 and 5. These are presented in small ξ variables. The plots are clearly asymptoting to their plume values for the various Prandtl numbers. There is also clear evidence of the asymptotic limit as $\sigma \to \infty$ a feature which was exploited by Haaland and Sparrow [4]. No such limit appears for decreasing values of the Prandtl number. One may also deduce from Figs. 4 and 5 that the plume state is more rapidly achieved as the Prandtl number increases. This feature

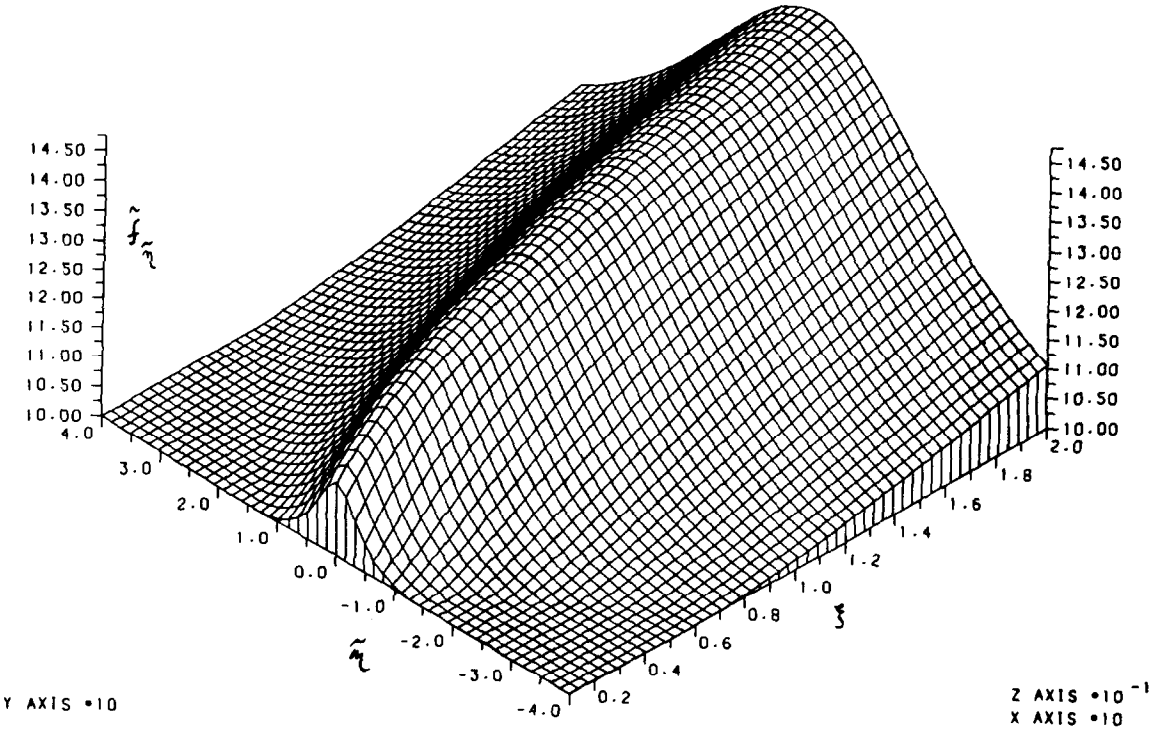

FIG. 1(a). Velocity profile development, $\sigma = 0.1$.

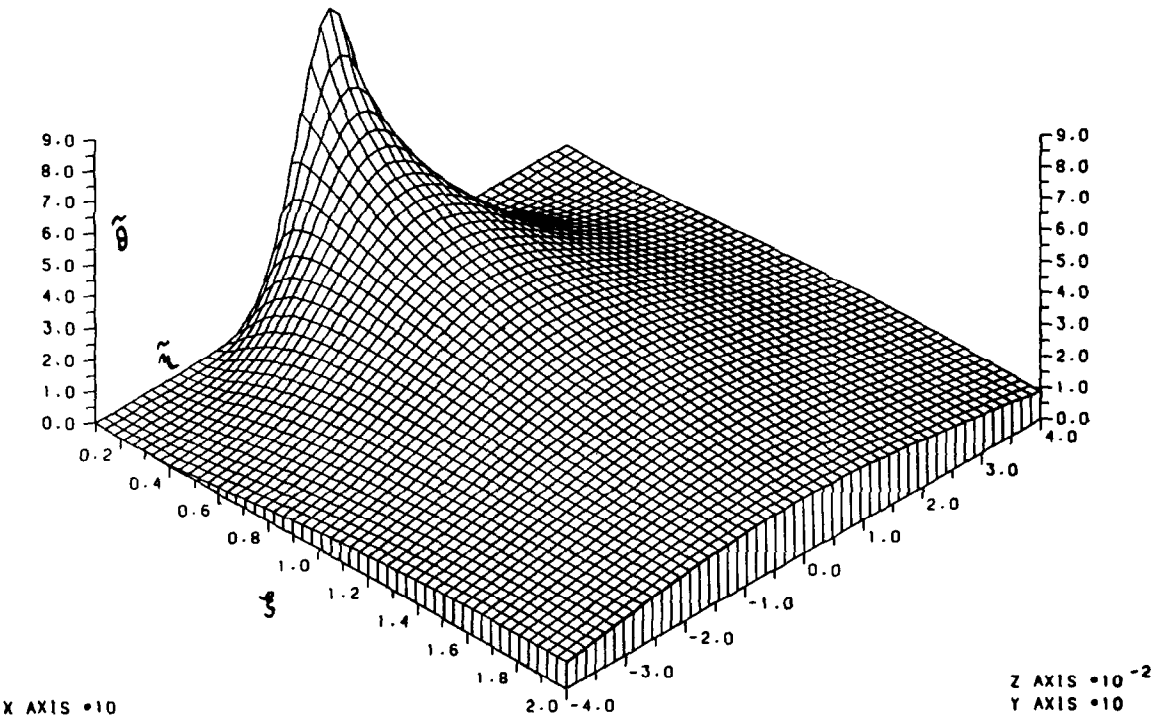

FIG. 1(b). Temperature profile development, $\sigma = 0.1$.

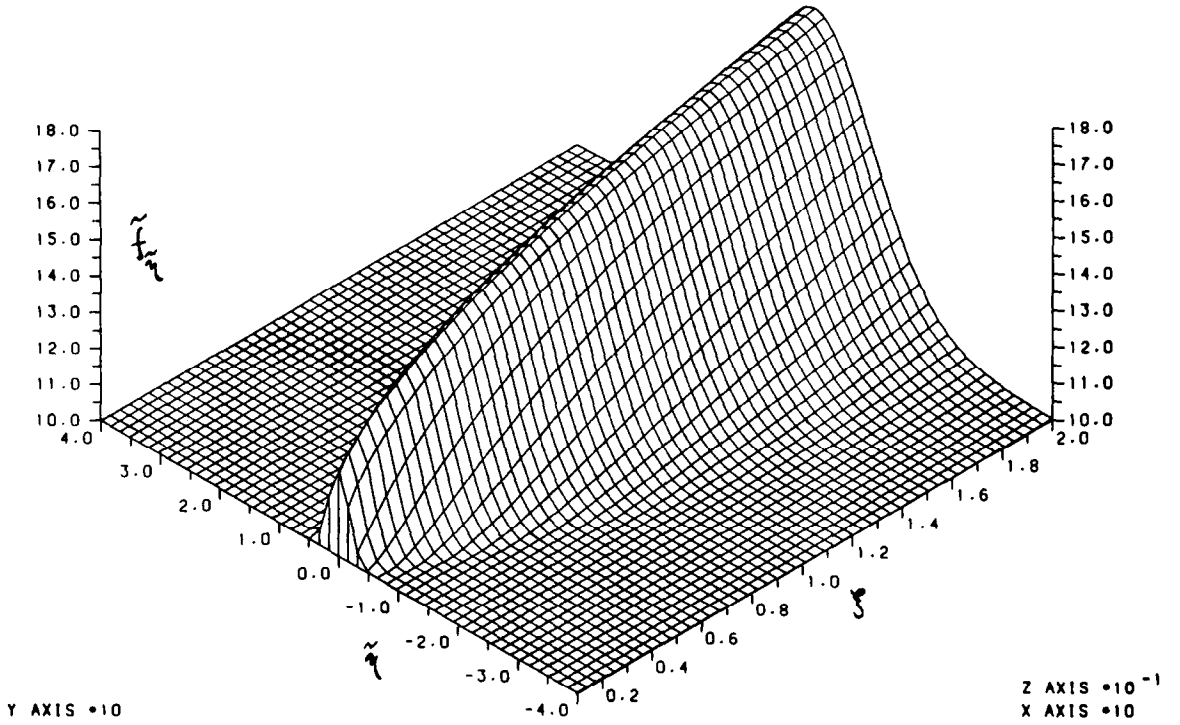

FIG. 2(a). Velocity profile development, $\sigma = 1$.

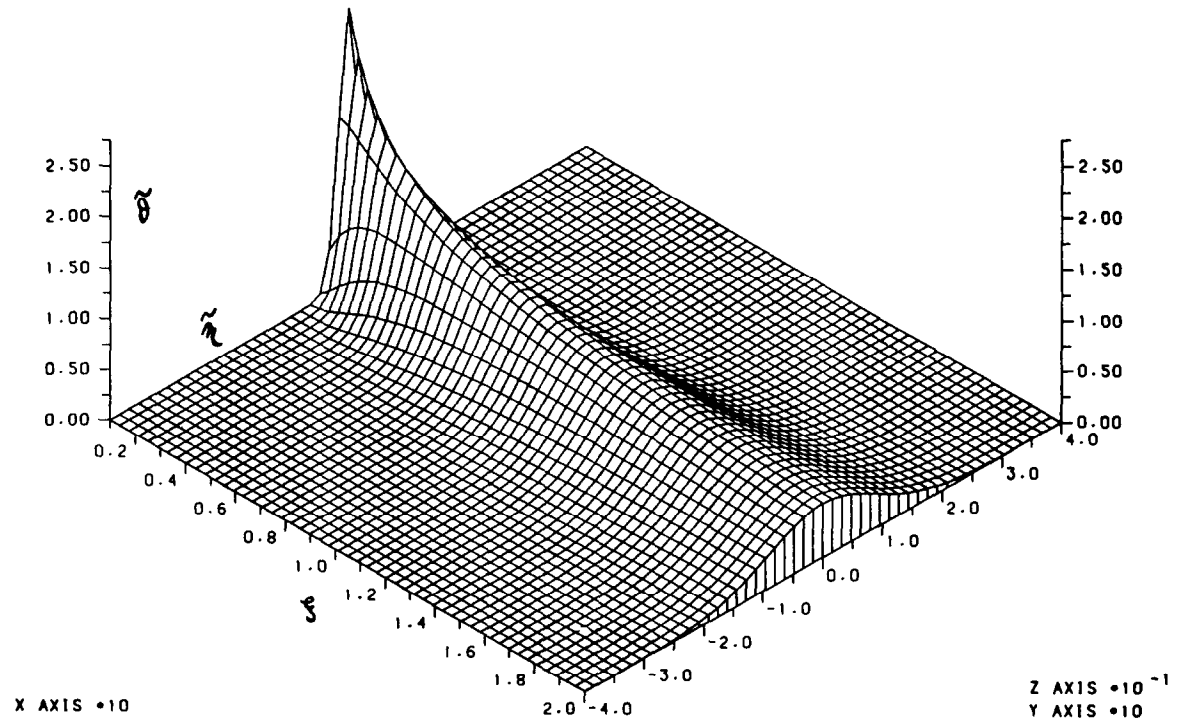

FIG. 2(b). Temperature profile development, $\sigma = 1$.

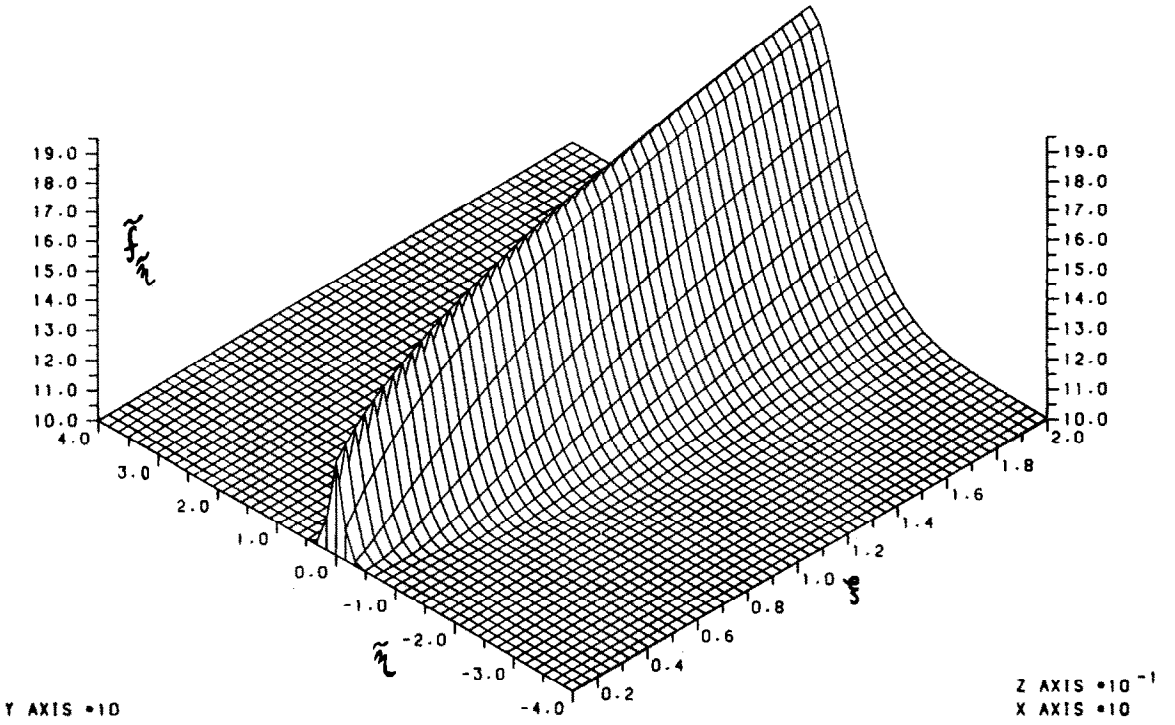

FIG. 3(a). Velocity profile development, $\sigma = 10$.

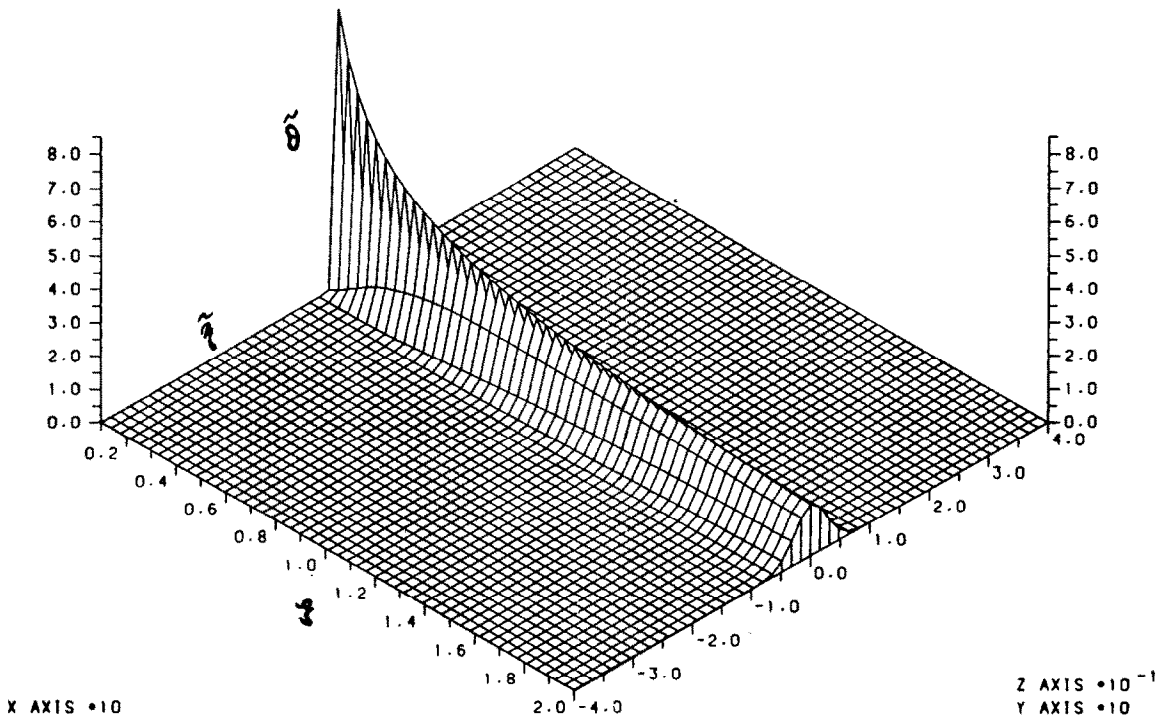

FIG. 3(b). Temperature profile development, $\sigma = 10$.

Table 1. Comparison between the pure free convection plume results of Fujii *et al.* [6] and the present computations at large ξ

σ	Fujii *et al.* $f_\pi(\infty,0)$	Wilks and Hunt $f_\pi(10^{20},0)$	Fujii *et al.* $\theta(\infty,0)$	Wilks and Hunt $\theta(10^{20},0)$	Fujii *et al.* $f(\infty,\infty)$	Wilks and Hunt $f(10^{20},\infty)$
0.01	0.5276	0.52742	0.7214	0.72083	9.64	9.706
0.03	0.61745	0.61771	0.64257	0.64330	6.40	6.281
0.1	0.71033	0.71033	0.56415	0.56416	3.944	3.940
0.3	0.77544	0.77544	0.49539	0.49540	2.654(5)	2.654
5/9	0.80093	0.8009303	0.45901	0.4590130	2.192(5)	2.192133
0.7	0.80872	0.80871	0.44616	0.44616	2.059	2.059
1	0.81937	0.81937	0.42753	0.42754	1.892	1.891
2	0.837485	0.8374843	0.396760	0.3967611	1.6709	1.670868
3	0.84747	0.84746	0.38240	0.38240	1.589(5)	1.589
5	0.85968	—	0.36786	—	1.519(5)	—
10	0.87516	0.87515	0.35336	0.35336	1.459	1.459
30	0.89547	0.89547	0.33889	0.33890	1.409	1.408
100	0.91095	0.91095	0.33018	0.33019	1.383	1.382
∞	0.93356	—	0.31983	—	1.346	—

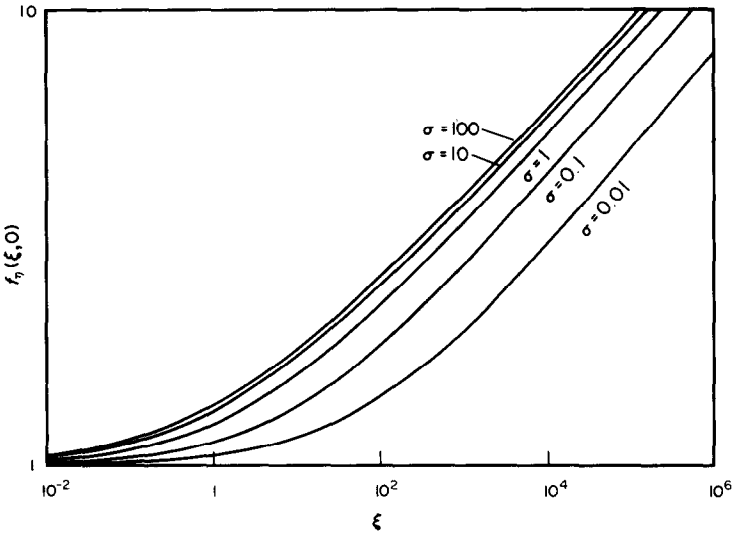

FIG. 4. Centre-line velocities.

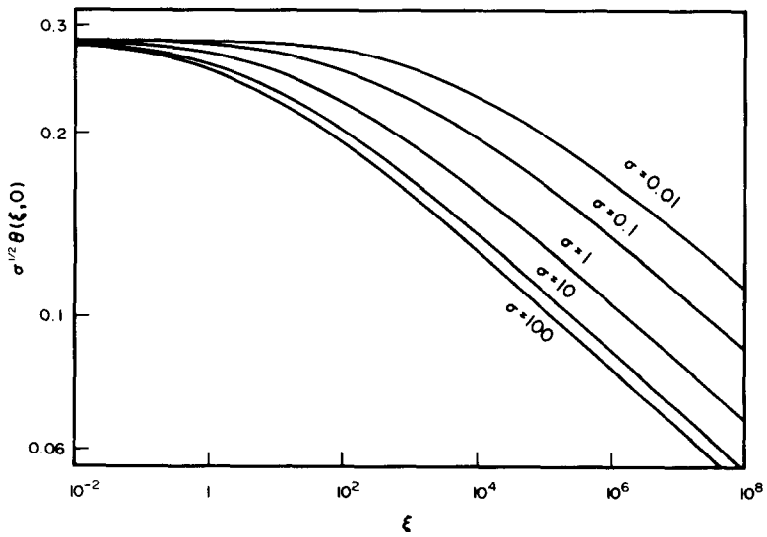

FIG. 5. Centre-line temperatures.

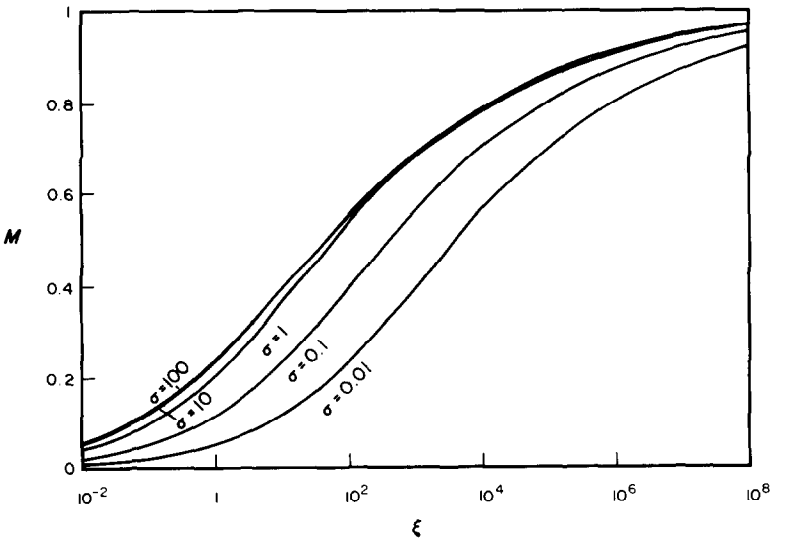

FIG. 6. Excess mass flux relative to fully developed plume flow.

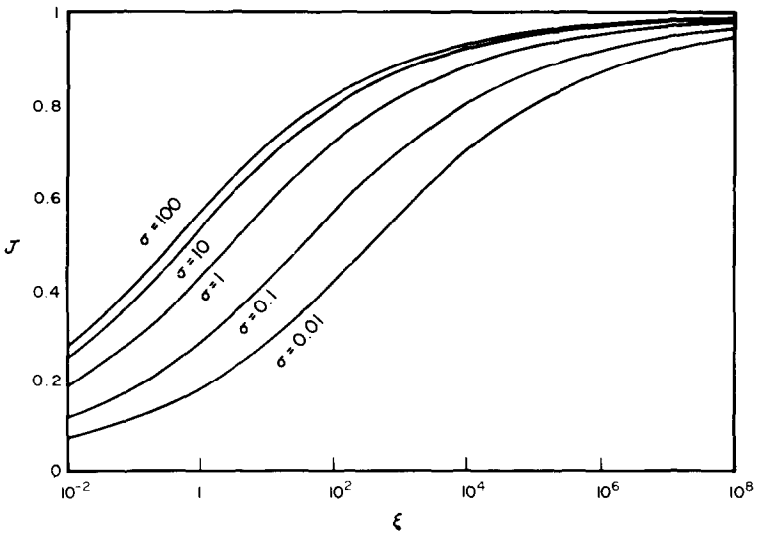

FIG. 7. Excess momentum flux relative to fully developed plume flow.

may be further quantified by examining (i) the excess mass flux as a result of the heat source normalized with respect to the plume mass flow rate, namely

$$M = \frac{\int_{-\infty}^{\infty} \rho(u - U_\infty)\,\mathrm{d}y}{\left\{\int_{-\infty}^{\infty} \rho u\,\mathrm{d}y\right\}_{\text{for plume}}} \tag{16}$$

$$= \frac{\xi^{1/2}\int_0^{\infty}\left[(1+\xi)^{1/10}\bar{f}_{\bar{\eta}} - \dfrac{1}{(1+\xi)^{1/10}}\right]\mathrm{d}\bar{\eta}}{\xi^{3/5}\{\bar{f}(\infty)\}_{\text{for plume}}} \tag{17}$$

and (ii) the excess momentum flux normalized with respect to the pure plume momentum, namely

$$J = \frac{\int_{-\infty}^{\infty} \rho u(u - U_\infty)\,\mathrm{d}y}{\left\{\int_{-\infty}^{\infty} \rho u^2\,\mathrm{d}y\right\}_{\text{for plume}}} \tag{18}$$

$$= \frac{\xi^{1/2}\int_0^{\infty}(1+\xi)^{1/10}\bar{f}_{\bar{\eta}}[(1+\xi)^{1/5}\bar{f}_{\bar{\eta}} - 1]\,\mathrm{d}\bar{\eta}}{\xi^{4/5}\left\{\int_0^{\infty}\bar{f}_{\bar{\eta}^2}\,\mathrm{d}\bar{\eta}\right\}_{\text{for plume}}}. \tag{19}$$

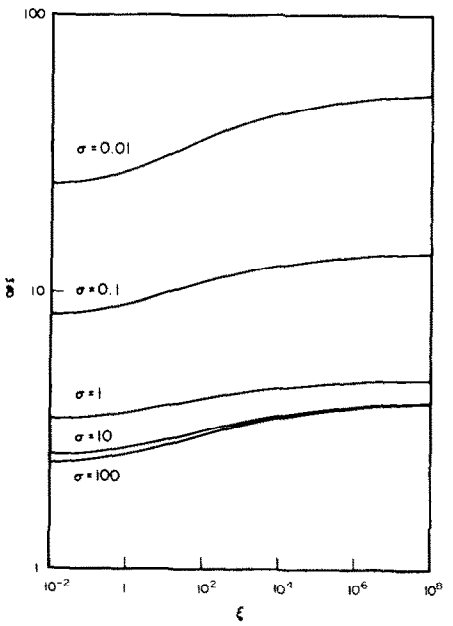

FIG. 8. Velocity half-width.

These quantities are illustrated in Figs. 6 and 7. Each curve approaches the asymptote unity as $\xi \to \infty$ as required by the definition. The figures provide confirmation of the approach to the plume state at lesser values of ξ for increasing Prandtl numbers. They may also be used to estimate the location at which the plume state has been achieved to within a prescribed tolerance.

Finally in Figs. 8 and 9 we present measures of the widths of the regions of velocity and temperature variations relative to free stream conditions, $\bar{\delta}$ and $\bar{\delta}_T$, respectively. Following Haaland and Sparrow [4] the region of velocity variation is defined as that over which velocities are in excess of 5% of the velocity defect between centre-line and free stream values. Thus $\bar{\delta}$ is that value of $\bar{\eta}$ at which

$$\frac{(1+\xi)^{1/5}\bar{f}_{\bar{\eta}} - 1}{(1+\xi)^{1/5}(\bar{f}_{\bar{\eta}})_{\bar{\eta}=0} - 1} = 0.05. \tag{20}$$

Similarly the region of temperature variation is defined as that over which the temperature exceeds 5% of the temperature defect between centre-line and free stream values and $\bar{\delta}_T$ is then that value of $\bar{\eta}$ for which

$$\frac{\bar{\theta}}{(\bar{\theta})_{\bar{\eta}=0}} = 0.05. \tag{21}$$

The ordinate of Fig. 9 has been scaled with respect to $\sigma^{1/2}$ in view of the known analytic form at $\xi = 0$.

5. NEGATIVE BUOYANCY

To investigate the flow when buoyancy forces are adverse with respect to the oncoming stream the equations appropriate to the transformations of equations (9) must be used, namely

$$f_{\eta\eta\eta} + \frac{1}{2}ff_{\eta\eta} - \xi^{1/2}\theta = \xi[f_\eta f_{\xi\eta} - f_\xi f_{\eta\eta}] \tag{22}$$

$$\frac{1}{\sigma}\theta_{\eta\eta} + \frac{1}{2}[\theta_\eta f + \theta f_\eta] = \xi[f_\eta\theta_\xi - f_\xi\theta_\eta]. \tag{23}$$

The boundary conditions are unchanged and the conservation constraint remains valid. The negative buoyancy is reflected in the sign of θ and the coefficient $\xi^{1/2}$ characterizes the flow as a developing perturbation about the uniform stream at $\xi = 0$.

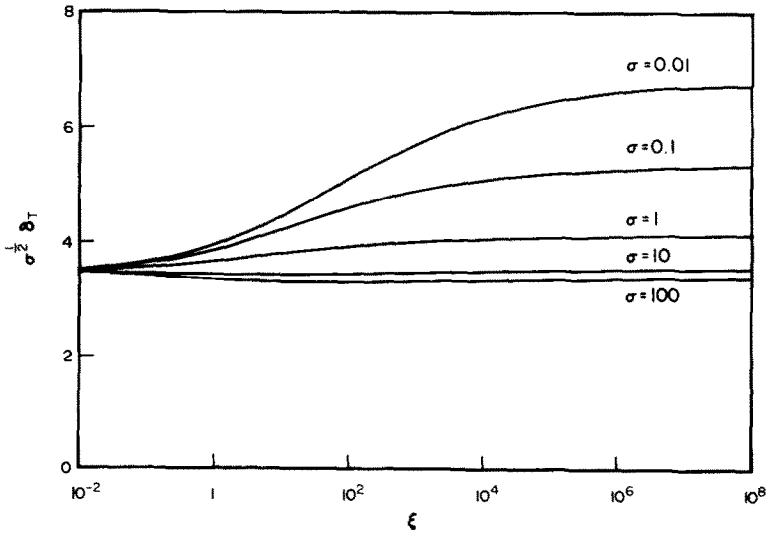

FIG. 9. Temperature half-width.

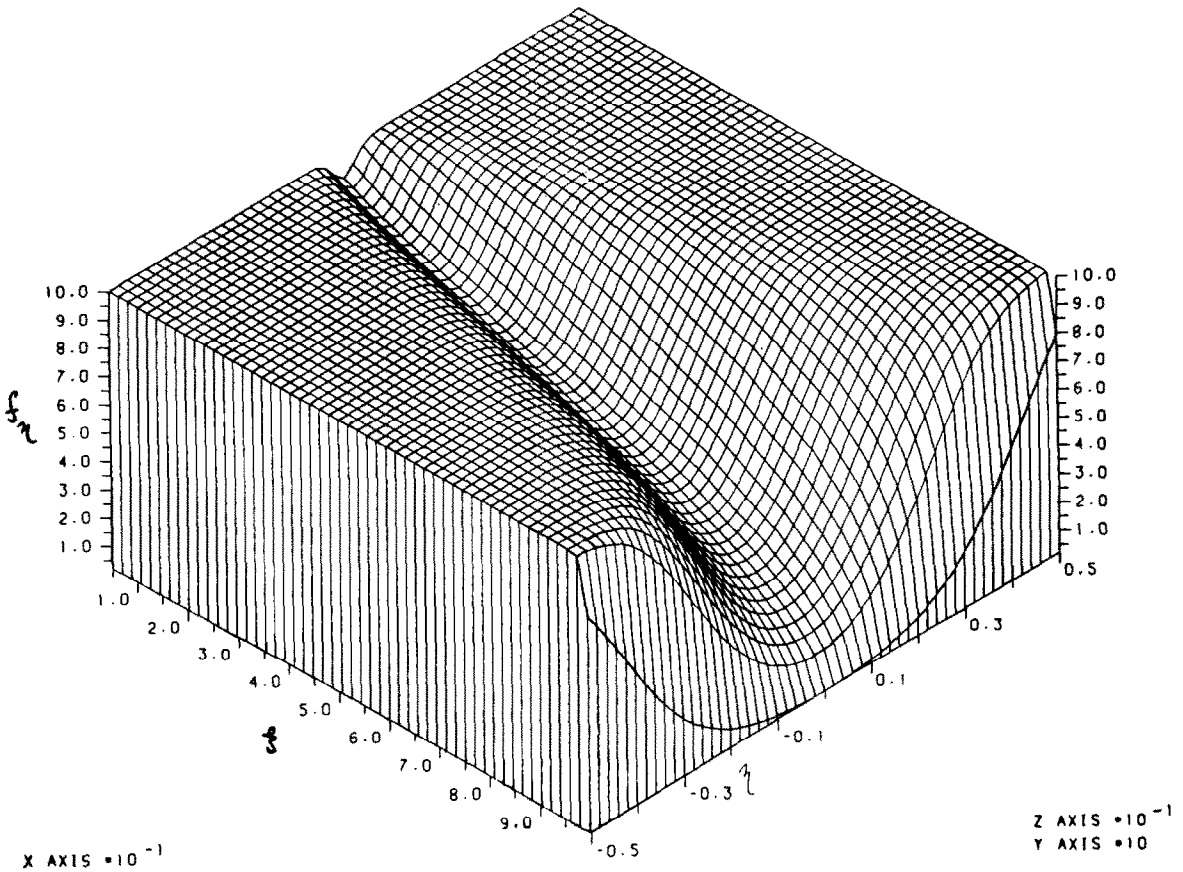

FIG. 10(a). Velocity profiles for negative buoyancy—View A, $\sigma = 1$.

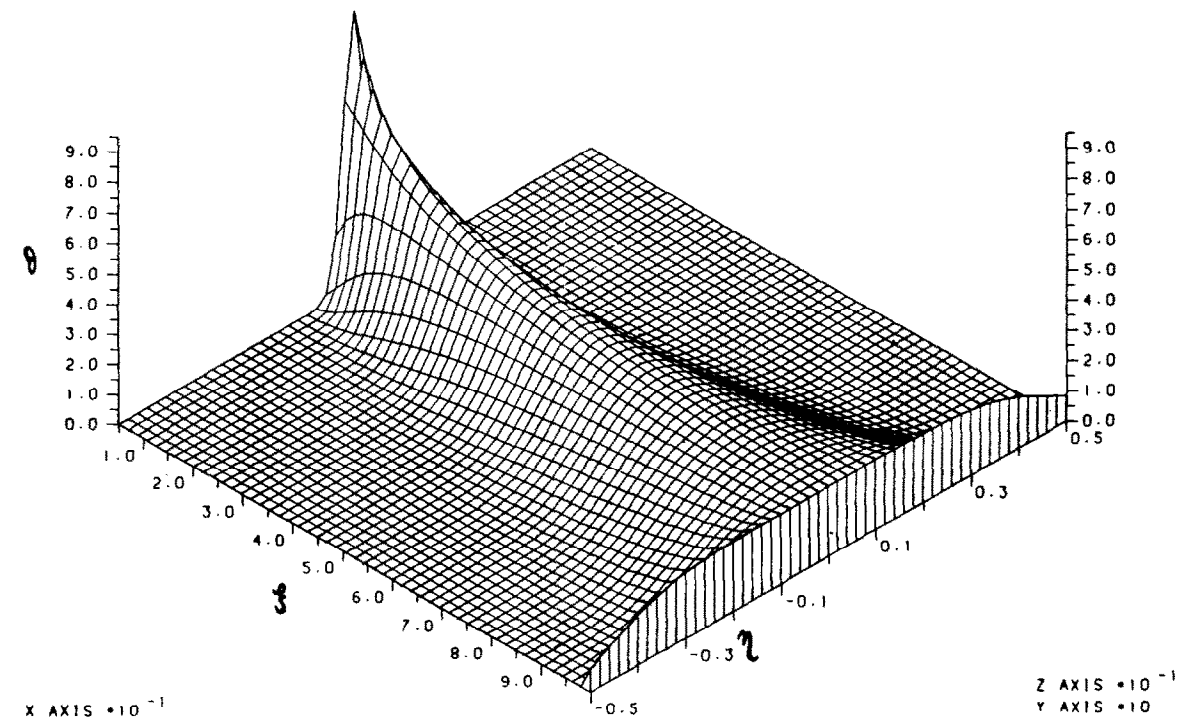

FIG. 10(b). Temperature profiles for negative buoyancy—View A, $\sigma = 1$.

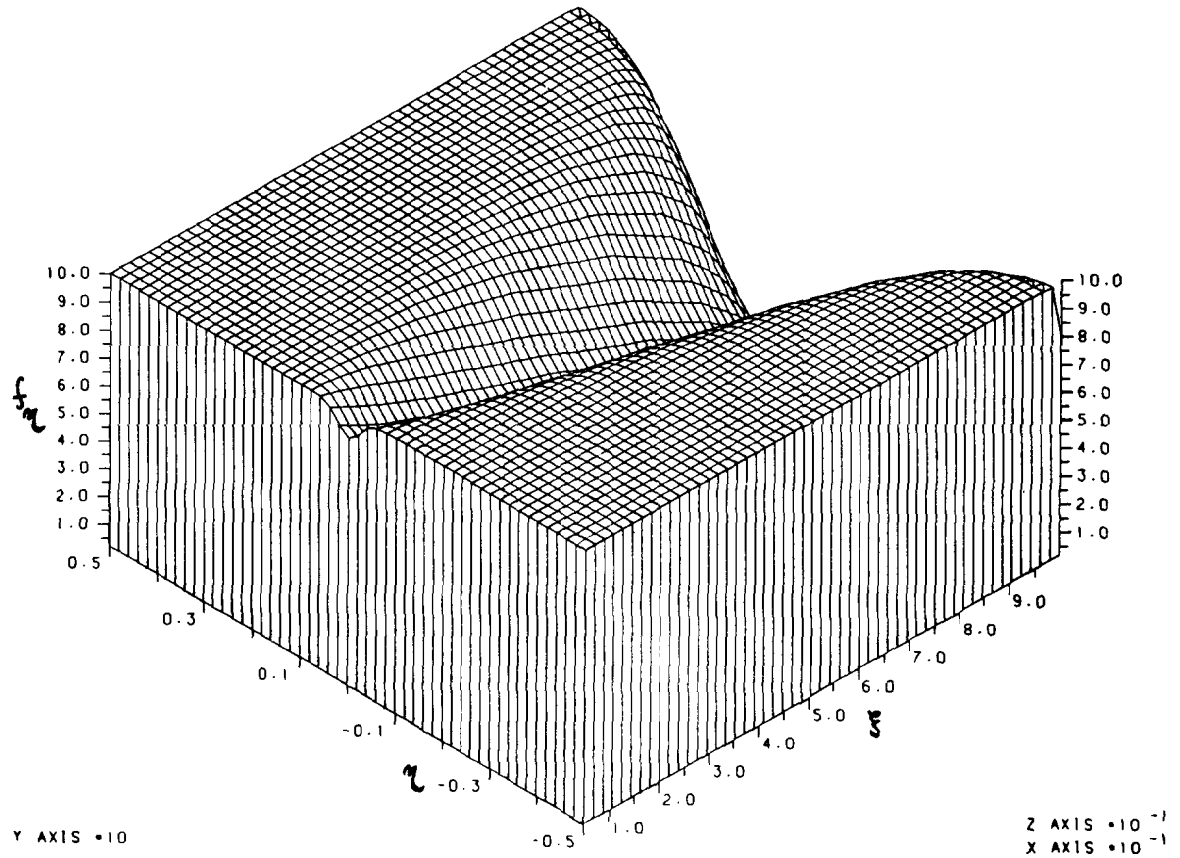

FIG. 10(c). Velocity profiles for negative buoyancy—View B, $\sigma = 1$.

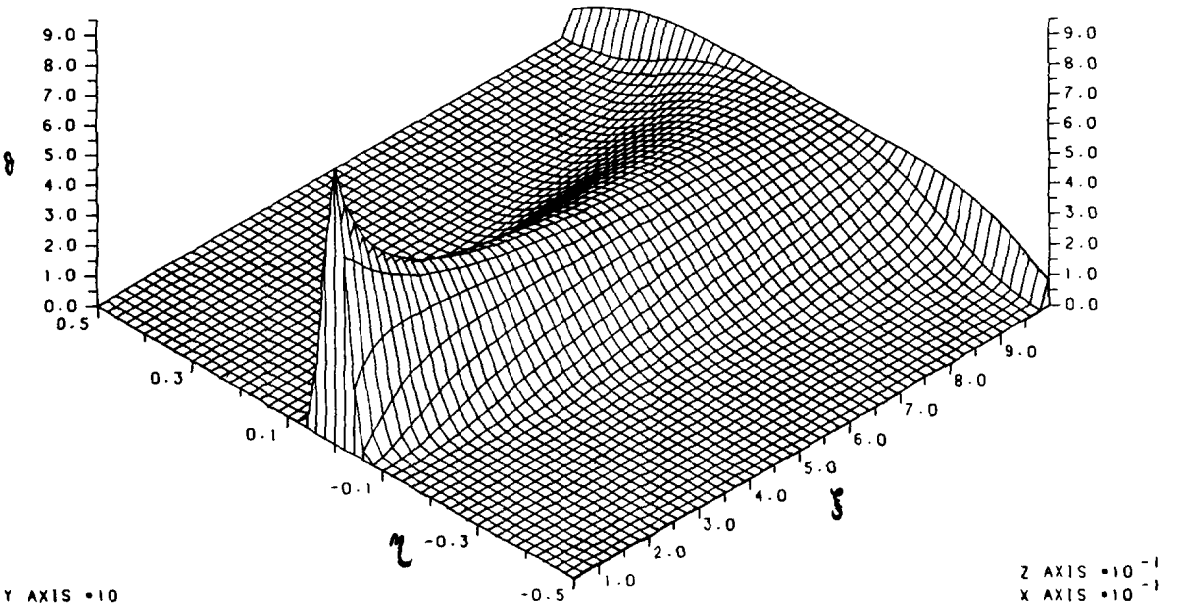

FIG. 10(d). Temperature profiles for negative buoyancy—View B, $\sigma = 1$.

The equations have again been integrated using the Keller box method. An indication of the features displayed by the computations is given in the series of illustrations in Figs. 10(a)–(d). These relate to the case $\sigma = 1$ and present the same information from two viewpoints. Note the singular behaviour of the centre-line velocity whilst the centre-line temperature remains of $O(1)$. As the singularity is approached the respective velocity and temperature regions of influence grow unboundedly. The temperature distribution develops towards a constant value over the central region of the stagnating plume. There is clearly no evidence of the temperature maximum suggested by Afzal [1]. Further detailed examination of the numerical results indicate that as the stagnation singularity is approached the displacement of maximum shear and maximum temperature gradient away from the axis of symmetry behaves as $\ln(\xi_s - \xi)$ where ξ_s is the stagnation point. This information, together with the knowledge that the centre-line velocity behaves as $(\xi_s - \xi)^{1/2}$ should enable the precise analytic structure of the singularity within the framework of the governing equations to be identified. Such an investigation however is beyond the scope of this paper.

6. CONCLUDING REMARKS

Numerical solutions have been presented for the vertical mixed convection flow of a uniform stream about a horizontal line source of heating or cooling. When the resulting buoyancy forces are favourable relative to the oncoming stream a formulation has been introduced in which the similarity states of the pure jet and the pure free convection plume are automatically incorporated. Each state arises naturally with respect to the limiting values of a characteristic coordinate which reflects the local relative significance of buoyancy and inertia. Solutions have been presented for a comprehensive range of Prandtl numbers and features monitoring the development of the flow between the jet and the plume have been illustrated. An indication of the accuracy of the solutions has been displayed by comparison with available results for the free convection plume.

Parallel computations of the flow field when buoyancy forces are adverse to the oncoming stream have also been obtained. A stagnation flow is generated as anticipated but which displays singular behaviour as the stagnation point is approached. Characteristics of the singularity have been identified from the numerical solution.

REFERENCES

1. N. Afzal, Mixed convection in a two dimensional buoyant plume, *J. Fluid Mech.* **105**, 347–468 (1981).
2. W. W. Wood, Free and forced convection from fine hot wires, *J. Fluid Mech.* **55**, 419–438 (1972).
3. P. Wesseling, An asymptotic solution for slightly buoyant plume, *J. Fluid Mech.* **70**, 81–87 (1974).
4. S. E. Haaland and E. M. Sparrow, Mixed convection plume above a horizontal line source situated in a forced convection approach flow, *Int. J. Heat Mass Transfer* **26**, 433–444 (1983).
5. R. Hunt and G. Wilks, Continuous transformation computations of boundary layer equations between similarity regimes, *J. comp. Physics* **40**, 478–490 (1981).
6. T. Fujii, I. Morioka and H. Uehara, Buoyant plume above a horizontal line heat source, *Int. J. Heat Mass Transfer* **16**, 755–768 (1973).
7. H. B. Keller and T. Cebeci, Accurate numerical methods for boundary layer flows I. Two-dimensional laminar flows, *Proc. 2nd Int. Conf. Num. Meth. Fluid Dyn.*, Berkeley, California (1971).

CONVECTION MIXTE VERTICALE A PARTIR D'UNE SOURCE RECTILIGNE HORIZONTALE, EN CHAUFFAGE OU REFROIDISSEMENT

Résumé—La convection mixte verticale d'un écoulement uniforme autour d'une source rectiligne horizontale créant des effets d'Archimède, peut être caractérisée par une évolution entre un panache faible ou intense. L'appréciation du développement de l'écoulement fournit la base pour la bonne formulation du problème. A partir de cette analyse, des solutions sont obtenues pour un large domaine de nombres de Prandtl. La convection mixte verticale à partir d'une source rectiligne horizontale peut, sous l'effet de forces d'Archimède adverse, conduire à une stagnation. Des solutions numériques des équations de couche limite dans ce dernier cas révèlent que la stagnation est accompagnée par un comportement singulier caractérisé par une croissance illimitée de la couche de cisaillement.

GEMISCHTE KONVEKTIONSSTRÖMUNG UM EINE HORIZONTALE LINIENQUELLE BEI HEIZUNG ODER KÜHLUNG

Zusammenfassung—Die vertikale gemischte Konvektion einer gleichförmigen Strömung um eine horizontale Linienquelle, welche gleichsinnig wirkende Auftriebseffekte hervorruft, kann durch die Entwicklung zwischen einer schwachen und starken Konvektionsfahne charakterisiert werden. Diese Abschätzung des sich entwickelnden Strömungsfeldes gibt eine Grundlage für eine sinnvolle Formulierung des Problems. Für einen weiten Bereich der Prandtlzahl ergeben sich umfassende Lösungen innerhalb dieses Rahmens. Dagegen darf erwartet werden, daß die vertikale gemischte Konvektion um eine horizontale Linienquelle bei gegensinnig wirkenden Auftriebskräften schließlich zu Stagnation führt. Die numerischen Lösungen der Grenzschichtgleichungen für diesen entgegensinnigen Fall zeigen, daß die erwartete Stagnation durch ein singuläres Verhalten begleitet wird, das durch ein unbegrenztes Wachsen der Scherschicht gekennzeichnet ist.

ВЕРТИКАЛЬНОЕ СМЕШАННОКОНВЕКТИВНОЕ ТЕЧЕНИЕ У ГОРИЗОНТАЛЬНОГО ЛИНЕЙНОГО ИСТОЧНИКА НАГРЕВА ИЛИ ОХЛАЖДЕНИЯ

Аннотация—Вертикальная смешанная конвекция у горизонтального линейного источника, создающего подъемное течение, может характеризоваться развитием восходящего потока разной интенсивности. Оценка интенсивности развивающегося течения создает основу для математической постановки задачи. Аналитические решения этой задачи получены для широкого диапазона чисел Прандтля. Вертикальный поток, взаимодействуя со встречным подъемным течением, создает застойную зону. Численные решения уравнений пограничного слоя для этого случая показали, что затормаживание потока сопровождается сингулярностью, проявляющейся в виде неограниченного роста сдвигового слоя.